First direct detection of large polycyclic aromatic hydrocarbons on asteroid (162173) Ryugu samples: An interstellar heritage

Hassan Sabbah, Ghylaine Quitté, Karine Demyk, Christine Joblin

First Direct Detection of Large Polycyclic Aromatic Hydrocarbons on Asteroid (162173) Ryugu Samples: an Interstellar Heritage

Hassan Sabbah[1*(0000-0001-5722-4388)], Ghylaine Quitté[1(0000-0002-7370-5859)], Karine Demyk[1(0000-0002-5019-8700)], Christine Joblin[1*(0000-0003-1561-6118)]

[1]IRAP, Université Toulouse III - Paul Sabatier (UT3), CNRS, CNES, 31028 Toulouse Cedex 4, France

*Corresponding author: hassan.sabbah@irap.omp.eu and christine.joblin@irap.omp.eu

Key Points:

- First direct detection of free aromatic species of large sizes with up to 61 carbon atoms in primitive extraterrestrial matter by applying a highly sensitive two-step laser mass spectrometry analysis to grain samples from the carbonaceous asteroid Ryugu (Hayabusa2 mission).
- First direct support for the interstellar polycyclic aromatic hydrocarbon (PAH) hypothesis, according to which large free PAHs are responsible for the aromatic emission bands that are major infrared features currently observed by the James Webb Space Telescope.
- The large aromatic species detected are present in trace amounts and future research is needed to develop sensitive techniques for studying these compounds in sample return missions and meteorites.

Keywords: PAHs, Asteroid Ryugu, Carbonaceous Chondrites, laser mass spectrometry, interstellar medium

ABSTRACT

Polycyclic aromatic hydrocarbons (PAHs) are considered major players in the physics and chemistry of star- and planet-forming regions. The interstellar PAH hypothesis is based on our understanding of the origin of the aromatic infrared bands (AIBs), a set of bright emission features that are now the focus of observations by the James Webb telescope. While AIB carriers are expected to be large free PAHs (50 carbon atoms or more), laboratory analysis of primitive carbonaceous chondrites (CCs) has mainly revealed relatively small PAHs, up to 24 carbon atoms. In this study, we present a comprehensive analysis of aromatic species in bulk samples from the carbonaceous asteroid Ryugu using a surface mass spectrometry technique provided by two-step laser desorption ionization. The resulting molecular distribution differs significantly from that obtained for a sample from the CC Orgueil, revealing aromatic species extending up to 61 carbon atoms. The species identified are composed of both peri-condensed PAHs and non-condensed aromatics. These results directly support the interstellar PAH hypothesis and open up new perspectives on the formation and evolution of organic matter in star-forming regions and in the solar nebula.

INTRODUCTION

In December 2020, the Hayabusa2 probe successfully returned samples from the surface of the carbonaceous (C-type) asteroid Ryugu. This in-situ sampling method ensures that scientists have access to pristine material, bypassing potential modifications related to atmospheric entry, contamination on Earth, and shock-related effects from meteoroid ejection events. The physical and chemical properties of Ryugu have been extensively studied, including its mineralogy, elemental composition, and organic content[1–4]. Various extraction methods were used to isolate specific organic fractions from Ryugu samples, and a range of analytical techniques were employed. These analyses unveiled a diverse assortment of organic compounds, such as amino acids, nucleobases, monocarboxylic acids, sugars, polycyclic aromatic hydrocarbons (PAHs), and other nitrogen-containing heterocyclic compounds[2,5]. These studies provide essential information about the early solar system and how organic matter was redistributed and evolved in different environments, including the primitive Earth.

Astronomers generally define interstellar PAHs as the carriers of the aromatic infrared bands (AIBs), which are extensively observed in various astrophysical environments rich in ultraviolet (UV) photons [6,7] such as photodissociation regions associated with massive star-forming regions, evolved stars (planetary nebulae), protoplanetary disks, and the diffuse interstellar medium (ISM). AIBs are now being studied in unprecedented detail thanks to the James Webb Space Telescope[8]. AIB emission is triggered by the absorption of UV photons from stars with energies up to 13.6 eV. Large (50 or more carbon atoms) and compact PAHs are therefore expected to dominate the emission because of their increased photo-stability[9,10]. In addition, advances in radio astronomy have made it possible to detect specific small PAHs with two cycles, namely indene (c−C_9H_8)[11,12] and cyano-naphthalene ($C_{10}H_7CN$)[13] in the TMC-1 dark cloud. This raises the question of the potential chemical link between these small PAHs present in regions protected from UV irradiation and the large PAHs that are the survivors in UV-irradiated regions[14].

Various analytical techniques have revealed the presence of PAHs in diverse types of primitive carbonaceous chondrites (CCs)[15,16]. In these objects, two isomers of $C_{16}H_{10}$, fluoranthene and pyrene, along with phenanthrene ($C_{14}H_{10}$), have been identified as the most abundant compounds[17]. However, it is noteworthy that the largest PAHs identified in meteorites are relatively small, consisting of only 24 carbon atoms (such as coronene). As the solar system

originated from a molecular cloud formed by the condensation of diffuse clouds, one would expect AIB carriers to be part of the building blocks of the solar system. As with presolar grains[18], we can expect these species to be better preserved in primitive bodies such as CCs, which have undergone the fewest changes since their formation in the solar system. This proposal finds support in the case of the fullerene C_{60} and its cation C_{60}^+, which have been detected in the diffuse ISM and various stellar environments[19–21]. In addition, the presence of C_{60} and other fullerenes was recently confirmed in the Almahata Sitta meteorite[22].

The case of C_{60} motivates the search for large PAHs in extraterrestrial carbonaceous matter, in order to support a scenario in which these species are the carriers of the AIBs and were inherited from the diffuse ISM. In this study, we carry out a specific molecular analysis to search for large free PAHs in bulk samples from the carbonaceous asteroid Ryugu and compare our results with those obtained from the Orgueil and Murchison carbonaceous chondrites.

EXPERIMENTAL METHODS

The AROMA setup

The AROMA (Astrochemistry Research of Organics with Molecular Analyzer) setup was designed with a specific focus on investigating the carbonaceous molecular composition found in meteorites and cosmic dust analogues[23]. The two-step laser mass spectrometry (L2MS) used here is a sensitive surface technique for various species such as PAHs, fullerenes, carbon clusters, and hydrogenated carbon clusters, as demonstrated in our previous work[22,24]. The setup consists in a microprobe laser desorption ionization source and a segmented linear quadrupole ion trap connected to an orthogonal time of flight mass spectrometer (o-TOF). Ions are produced at low background pressure (10^{-6} mbar). At first, a pulsed (5 ns) infrared laser (Nd:YAG at 1064nm) is focused on the sample with a spot size of 300 µm to cause rapid and localized heating and therefore to promote desorption. Typical laser desorption laser fluence and irradiance for this work are 150 mJ/cm^2 and 30 MW/cm^2, respectively. In a second step, a pulsed (5 ns) ultraviolet laser (fourth harmonic of an Nd:YAG at 266 nm) intercepts perpendicularly the expanding plume of the desorbed molecules. This leads to selective ionization of molecules that can undergo (1+1) resonance-enhanced multiphoton ionization (REMPI) such as fullerenes and aromatic species. Laser ionization fluence and irradiance for this work are 16 mJ/cm^2 and 3.2 MW/cm^2, respectively. Aliphatic species are usually not observed using REMPI at 266 nm. However, a contribution from other ionization processes is possible. In particular, the interaction of the IR (1064 nm) laser with the sample matrix and/or the substrate is, in our laser fluence conditions, capable of producing atomic ions from metal and mineral phases as we reported earlier[22,25]. This interaction may generate ions independently of the L2MS scheme, as is the case in experiments using SALDI (Surface-assisted laser desorption/ionization)[26]. This likely explains why we observe a limited number of aliphatics in our experiments, as presented here.

Molecular family analysis

For each detected m/z peak with a signal-to-noise ratio (S/N) greater than 10, a chemical formula is assigned using the mMass software, an open-source mass spectrometry tool[27]. For each peak, mMass proposes a number of species from which we select the one with the highest aromaticity and the smallest difference between the position of the recorded peak and the exact mass within the mass accuracy of our instrument, which we know to be at least 0.01 m/z. We initially assigned pure hydrocarbons, but in the process identified a number of cases where species containing heteroatoms (N, O) appear to be better candidates (see for instance Fig. S1). Our o-TOF mass spectrometer achieves a mass resolution (m/Δm) of 10 000 at m/z 202 and up

to 15000 at m/z 262, which is not sufficient to separate two species whose mass differs by 0.012 m/z (difference between N and CH_2). However, it does have the mass accuracy needed to conclude that a N-containing species is present if there is no dominant pure hydrocarbon peak nearby. We calculated an average value for the difference between the positions of the peaks and the exact masses of the assigned species. This value is 0.0000±0.0106 if we include all the peaks analyzed and -0.0005 ± 0.005 if we only consider the species containing at least one atom of N. We can see that the assignment of the latter species is more accurate, which may be due to the fact that we consider these species as alternatives to pure hydrocarbons only in specific cases where a clear assignment could be made (typically the pure hydrocarbon peak having a higher mass of at least 0.010 m/z). This also corresponds to cases in which contamination by the hydrocarbon peak is minimized. Using this method, we were able to identify about 250 hydrocarbons, including large aromatics with nitrogen, and dozens of species containing oxygen and both nitrogen and oxygen. We stress that our mass assignment is best guess and that a complete assignment of organic formulae with CHNO would require a resolution greater than 100,000 at m/z 202.

We then calculate the double bond equivalent (DBE)[28] for each molecular formula. This is achieved using the following equation for a given chemical formula

$$DBE = C\# - H\#/2 + 1 \quad (1)$$

with C# and H#, the number of C and H atoms in the identified pure hydrocarbons molecules, respectively. The DBE is equal to the number of rings plus double bonds involving carbon atoms (because each ring or double bond results in a loss of two hydrogen atoms). It allows us to sort the detected ions into families of compounds. Pure carbon species are sorted into C clusters (C# < 30) and fullerenes (C# ≥ 30). It has been established that a hydrocarbon compound should contain an aromatic cycle if its aromaticity index (AI) defined by the DBE/C# ratio exceeds the limit of 0.5[29]. Similarly, AI values larger than 0.67 are indicative of a condensed structure. Aromatic compounds are molecules that contain at least one benzene ring, while condensed aromatics are molecules that contain multiple rings fused together (PAH-like structures). Peri-condensed PAHs have at least one carbon atom that is shared by three rings. This creates a more compact and interconnected structure (e.g., pyrene, coronene, and ovalene). Cata-condensed PAHs have no carbon atom sharing more than two aromatic rings. This results in a more linear and extended structure (e.g., anthracene and chrysene). A value of AI=0.9 is the limit predicted by Hsu et al.[30] above which an aromatic planar molecule could not exist. In our analysis, we call HC (Hydrogenated Carbon) clusters hydrocarbons with AI > 0.9. Aliphatics species are the ones with AI < 0.5. For hydrocarbon containing nitrogen or oxygen the general formula of AI is used:

$$AI = (1+C\#-O\#-S\#-0.5H\#)/(C\#-O\#-S\#-N\#-P\#)[29] \quad (2)$$

with O#, N#, P# and S#, the number of O, N, P and S atoms in the identified organic molecules, respectively

RESULTS:

L2MS analysis of Ryugu samples

We conducted a molecular analysis directly on the intact grain C0083_1 collected during the second touchdown of the Hayabusa2 mission on the asteroid Ryugu. This grain is sourced from collection chamber C and measures approximately 1 mm (Figure 1a and 1b). In addition, we

prepared two powder samples from the same grain (Figure 1c), designated C0083_1P1 and C0083_1P2 (Figure 1d), by pressing fragments (sub-mm in size) of C0083_1 with ceramic tweezers onto copper double tape, resulting in a uniform, smooth powder. We note that the mechanical contact with the tweezers was enough to reduce the fragment grain into powder. All samples underwent L2MS analysis using the AROMA setup (see Experimental methods). Figure 2 depicts the recorded mass spectra in the m/z range from 100 to 800. The predominant mass peaks fall between m/z 100 and 300, with the highest peak identified at m/z 191.08 ($C_{15}H_{11}$) for C0083_1 and m/z 202.08 ($C_{16}H_{10}$) for C0083_1P1 and C0083_1P2.

In the mass spectra of all three samples (C0083_1, C0083_1P1, C0083_1P2), we identified the peaks of 12 typical PAHs containing between 10 and 24 carbon atoms ($10 \leq C\# \leq 24$; m/z range from 128 to 302). The relative peak intensities exhibit a noteworthy similarity across the three samples (Figure S2). However, the smallest species ($C\# \leq 14$) are less abundant on the surface of the studied grain compared to the powders, particularly with respect to P1. Notably, the absence of detection of $C_{10}H_8$ for C0083_1 suggests a preferential depletion of the smallest PAHs on the grain's surface probably due to their higher vapor pressure.

While 90% of the peaks detected in the intact grain are also present in the mass spectra of the powder samples, a larger number of peaks and more intense peaks are evident in the powders (Figure 2). The highest mass detected in the intact grain is at m/z 322.16 ($C_{25}H_{22}$) whereas several larger species are seen in the powders, extending up to m/z 800. L2MS being a surface technique, the powders provide a larger, more uniform, and smoother sample surface compared to the bulk grain. Additionally, the distribution of organics in such samples is naturally heterogeneous. Therefore, by spatially averaging the mass spectra from different zones, we can enable a more effective sampling of this heterogeneity. In the following, an average data set for the two samples C0083_1P1 and C0083_1P2 is considered and denoted C0083_P1P2.

Up to four hundred hydrocarbons have been identified in C0083_1P1P2, reaching sizes up to C# = 61. Figure 3 provides an overview of the sum of ion intensities and the total number of attributed chemical formulas categorized per C#. Notably, the intensity experiences a drastic reduction for larger species (by a factor of approximately 50), whereas the number of detected species undergoes a more moderate decrease, typically around a factor of 5. Table 1 lists examples of chemical formulas for large species ($C\# \geq 30$) grouped per carbon number (C#) and guided by the diversity shown in Figure 3.

Molecular families and organic diversity in Ryugu samples

For further analysis of the identified species, the double bond-equivalent (DBE) method[28] was employed. DBE is indicative of the unsaturation level of molecules and serves to define an aromaticity index (AI)[29], as explained in the Experimental methods section. The AI diagram for pure hydrocarbons is given in Figure 4 and in Figure S3 for species containing nitrogen and oxygen. For simplification, the latter are labeled CHN, CHO and CHNO species. Figure 5 summarizes the sum of ion intensities and the total number of attributed chemical formulas for the eight families defined above. The bar charts unequivocally highlight the prevalence of condensed aromatics, followed by non-condensed aromatics, as delineated by the AI range specified above. Condensed aromatics proved to be the dominant species both in terms of ion intensity and number of species detected. However, the difference with the other species is greater when ion intensities are considered, which can be attributed to the optimized sensitivity of AROMA for the detection of condensed aromatics. CHN species is the third population both in total ion signal and in number of peaks annotated. This population contains a mixture of aliphatic, non-condensed aromatic, and condensed aromatic compounds as seen in Figure S3.

Aromatics in Ryugu samples compared to carbonaceous chondrites

As Ryugu is a type-C asteroid and Hayabusa2 samples have been shown to be similar to CI chondrites[31,32], we compared our results with those obtained on well-studied CCs, namely Murchison (CM2) and Orgueil (CI1). Our previous work using AROMA involved characterizing the molecular content of Murchison powder[23]. In the present study, Orgueil powder was analyzed. The aromaticity index of these two representative CCs is juxtaposed in Figure S4 with that of the C0083_1P1P2 data set.
We note that, for each analysis, fresh fragments of a few milligrams were crushed using a mortar and pestle. The powder, once uniform and smooth, was attached to a 10 mm disk of stainless steel with conductive copper tape. This method ensures consistent preparation of CCs and allows for a better comparison of the results. In powders, the surface from which species can be desorbed is increased and a better molecular sampling is achieved by moving the IR laser on the powder while recording the mass spectra, which minimizes the effect of sample heterogeneity on the results.

The predominant aromatic species identified in Murchison and Orgueil are found not to exceed C# = 25 and C# = 30, respectively, except for one species $C_{38}H_{16}$ in Orgueil. Figure 6 provides a view on the carbonaceous molecular families derived for Ryugu samples (C0083_1P1P2 data set) and for the samples of the two CCs, Murchison and Orgueil. The prevalence of condensed aromatic compounds is apparent across all samples. However, the Ryugu sample also contains a significant fraction of non-condensed aromatics, this fraction being larger in the small-to-medium size range ($6 \leq C\# < 30$). Figure 7 provides a general view of the mean hydrogenation of the molecular species detected as a function of C# for Orgueil and Ryugu samples. In general, species in Orgueil have a lower hydrogenation degree compared to Ryugu samples. For Orgueil, the mean hydrogenation degree is found to be at the limit of peri-condensed aromatics (see the experimental methods section), or more frequently, below this limit whereas it is well above for Ryugu. The species containing heteroatoms (N or O) are found to have a high hydrogenation degree in both Orgueil and Ryugu samples (Figure 7). Figure S5 displays the DBE vs C# plots in which the horizontal lines point to alkylated series[23], whereas vertical lines point to hydrogenated series. Pyrene/fluoranthene ($C_{16}H_{10}$) and their methyl-substituted forms have been already identified in Ryugu samples using solvent extraction and gas chromatography (GC) techniques[2,33]. Based on our data, the $C_{16}H_{10}$ peak and its related Cn-$C_{16}H_{10}$ alkylated species (with n ranging from 1 to 3) dominate in Ryugu samples (C0083_P1P2 data set). More generally, long series of alkylated species seem to be present in Ryugu, whereas this alkylation seems more limited in Orgueil.

A notable characteristic of Ryugu samples (C0083_1P1P2), when compared to Orgueil and Murchison, is the prevalence of a substantial number of aromatic species with $C\# \geq 30$. We have identified 122 aromatic species with $C\# \geq 30$, compared with 273 species with $C\# \leq 30$. The large aromatics constitute a significant portion of the total ion intensity attributed to aromatic species, typically around 5% (Figure 6).

DISCUSSION

Zeichner et al.[34] performed a ^{13}C isotope analysis on PAHs such as pyrene/fluoranthene and other smaller PAHs in Ryugu samples. They concluded that some PAHs come from cold temperature conditions typical of molecular clouds (~ 10K) and others from higher temperatures (> 1000K) that can be found in circumstellar environments or in the parent body. Based on the analysis of macromolecular organic matter in the Ryugu samples, Yabuta et al.[35] concluded that the organic matter was modified by aqueous alteration on the asteroid's parent body, but was not subjected to major heating events, with temperatures below 473K. Lecasble

et al.[36] have shown that PAHs are stable in simulated asteroidal hydrothermal conditions at 423K.

The L2MS analysis presented here provides a complementary view from previous analysis of the soluble and macromolecular organic matter in Ryugu samples [2,33–35]. As discussed earlier, we detected mass peaks that correspond to the major small and medium-size PAHs identified using gas chromatography–mass spectrometry (GC-MS) in Ryugu and in CCs[33]. In addition, a number of CHN species we were able to identify are common to those extracted in methanol and analyzed by nanoscale liquid chromatography/high resolution mass spectrometry[2]. From Fig. 6 of the latter article, covering the range m/z 266 to 294, we can list $C_{18}H_{27}N_2$, $C_{19}H_yN$ (y=24, 30, 32, 34), $C_{20}H_yN$ (y=24, 26) as common species. This comparison gives us some confidence in our ability to detect intact CHN species despite the used laser scheme and the limited mass resolution of AROMA. Naraoka et al.[2] also showed that $C_xH_yN_2$ are minor species compared to C_xH_yN (in the m/z range presented), which is consistent with our detection of a limited number of $C_xH_yN_2$ and only one $C_xH_yN_2O$ species (~20% of the total CHN+CHNO species identified), the largest species identified being $C_{18}H_{27}N_2$, $C_{19}H_{10}N_2$, $C_{20}H_{10}N_2$, $C_{20}H_{16}N_2$, $C_{24}H_{31}N_2$ and $C_{54}H_{40}N_2$.

Naraoka et al.[2] assigned the detected CHN species to alkylated N-containing heterocycles, in particular pyridine homologs. Our data supports the presence of N-containing heterocycles with three mass peaks observed with very high ion intensity: $C_{11}H_9N$ (2-phenylpyridine?), $C_{10}H_7N$ (1-ethynylindole?) and C_9H_7NO (8-hydroxyquinoline?). The presence of non-condensed species made of small aromatic domains with interconnected chains was also suggested by analysis of the XANES spectra of Ryugu grains[35]. As these species should be more fragile than condensed aromatics to interaction with lasers, it is possible that a certain number of ions detected in our experiments are fragments of larger non-condensed molecules. This also implies that these molecules have not been submitted to any significant thermal processing in the parent body. This reinforces the idea of the pristine nature of Ryugu material[35] compared to Orgueil and Murchison samples (Figure 7). This is in line with infrared spectroscopy measurements on organic-rich acid residues, generally referred as insoluble organic matter (IOM). The infrared spectra of Ryugu IOM reveal similar spectral signatures than those of the IOM of unheated CCs (such as Orgueil and Murchison) but with a higher aliphatic/aromatic ratio.[37]. Further studies would be required to determine if a connection exists between IOM phases and the non-condensed aromatics detected here in the bulk.

Unlike in the CC samples, we were able to detect in Ryugu samples large aromatic species with C# > 30, the largest identified being $C_{61}H_{44}$ and $C_{61}H_{47}NO$. Laser desorption ionization (LDI) coupled with ultra-high-resolution mass spectrometry has been used in previous studies to reveal the molecular content of the IOM in CCs[38,39]. These studies revealed the presence of large aromatic species with incorporated heteroatoms (nitrogen, oxygen, and sulfur). The authors could not conclude on the origin of these species. Danger et al.[38] pointed out the difficulty of extracting large aromatic structures both in LDI experiments, which required high laser power, and during the IOM preparation. reported that a high laser power was necessary to observe large aromatic structures, likely due to the difficulty to extract them both in the preparation of the IOM and in LDI experiments for which a relatively high laser power was used. Under these conditions, covalent bonds can be broken, making it difficult to conclude whether these species are present as free molecules in the IOM or are part of a larger macromolecular structure. This can explain why the species detected in LDI experiments were found with a H/C~0.5-0.6 whereas we detected large species with H/C up to 1 and even more (~1.2) for N-bearing species. The non-condensed CH species probably share a common origin

with the CHN species discussed above. However, we also detect CH species with much lower H/C~0.3-0.5, which likely correspond to peri-condensed structures (see Figure 4). The fraction of condensed species is found to increase with size (Figure 6). This is likely related to the sensitivity of our laser scheme to condensed aromatics relative to non-condensed ones. Furthermore, as mentioned above, the fragmentation of non-condensed species can limit the sizes that can be observed in the gas phase, whereas large condensed PAHs are known to be very stable under photon irradiation[10]. Large condensed PAHs are not detected in the bulk samples from Murchison and Orgueil, although the total ion signal of condensed aromatics is comparable within a factor of two in these samples and in those from Ryugu (C0083_1P1P2 data set). This highlights a difference in composition between Ryugu samples and the studied CCs. The size distribution shown in Figure 2 also suggests that we have only a partial view of the composition of these large species in the Ryugu samples and that more of them could be detected with greater sensitivity. Among the species detected, a large number correspond to peri-condensed structures (see Figure 4). Using AROMA on a variety of synthetic samples, we could find such large peri-condensed PAHs only in nascent soot particles[24]. There are indeed hundreds of common mass peaks between Ryugu powders and soot particles previously analyzed, with approximately 20 peaks corresponding to peri-condensed structures with C#≥30 (e.g., $C_{30}H_{12}$, $C_{32}H_{16}$, $C_{35}H_{16}$, $C_{36}H_{16}$, $C_{38}H_{16}$, $C_{39}H_{18}$, ..., $C_{48}H_{16}$) as listed in Table S1. The latter species are specific to the high-temperature chemistry and thermal processing observed in combustion processes[40].

Understanding the origin of the AIBs and their variations in astrophysical environments such as massive star-forming regions is a very active field in the JWST era[8]. It is generally accepted that the carriers of the AIBs are dominated by large free PAHs capable of converting the energy they absorb in the UV into IR photons. However, the PAH hypothesis runs up against certain difficulties, in particular the lack of spectral assignment of individual species. Our L2MS analysis of the Ryugu samples enabled us to detect large peri-condensed PAHs giving us the first direct access to plausible contributors to the AIB emission.

The way in which these PAHs are formed has not yet been elucidated. By analogy with flame chemistry, it has been proposed that PAHs could be formed in the envelopes of carbon-rich stars where sufficient temperature conditions can be found[41,42]. The common mass peaks detected in the L2MS analysis of Ryugu and nascent soot particles and corresponding to large peri-condensed PAHs suggest that these species originate from the circumstellar envelopes of evolved stars and could be considered as presolar circumstellar grains[43]. This point needs however to be further investigated knowing that a scenario of formation of large PAHs in circumstellar envelopes has not yet been proven, either observationally[7] or experimentally[44]. Another formation scenario was suggested from the analysis of the evolution of the AIBs in photodissociation regions associated with star-forming regions. In this scenario, AIB carriers would be produced by photo-processing of precursors, likely in the form of very small grains (nanometer-sized) or clusters[45] with a mixed aromatic and aliphatic composition[46]. As aliphatic bonds can be easily dissociated by UV photons, we do not expect such precursors to survive in the diffuse ISM and be incorporated in the solar nebula. Consequently, if species such as non-condensed aromatics are observed in Ryugu samples, they should have reformed in the molecular cloud at the origin of the solar nebula and been incorporated into the primitive bodies of the solar system without having been subjected to energetic conditions. The large non-condensed aromatic species detected in Ryugu samples could therefore shed light on the chemistry leading to the precursors of AIB carriers in molecular clouds.

CONCLUSION

We detected large free aromatic species in primitive material of the solar system provided by Ryugu samples using a highly sensitive L2MS analysis. This work opens up new prospects for the study of PAHs in star- and planet-forming regions and the contribution of these molecules to the AIBs, which are key features at the JWST era. Much remains to be understood about PAH formation scenarios in these environments. In addition, the search for these species in the organic matter of CCs and C-type asteroids should give us a better understanding of the interstellar heritage of the early solar system. At this stage, the large aromatic species are detected at trace levels, and future research is needed to develop sensitive techniques for studying these compounds in sample return missions and meteorites.

Ethics statements

The authors confirm that they have followed the ethical policies of the journal.

Conflict of interest

The authors declare no conflict of interest.

Data availability

Mass spectrometry data and chemical analysis tools for all the studied samples are made publicly available in the AROMA database: http://aroma.irap.omp.eu

Acknowledgements

We thank the JAXA (the Japan Aerospace Exploration Agency) curation center for providing us with the Ryugu samples through the Announcement of Opportunity available at https://jaxa-ryugu-sample-ao.net. The obtained results would not have been possible without this cooperation with JAXA. We thank the European Research Council for funding support under Synergy Grant ERC-2013-SyG, G.A. 610256 (NANOCOSMOS). This work also benefited of the state funding operated by the Agence Nationale de la Recherche as part of the France 2030 scheme, ORIGINS PEPR Program, μL2-HRMS project with grant number ANR-22-EXOR-0009.

Author contributions

H.S., G.Q., and C.J. conducted L2MS experiments. H.S. and C.J. performed mass spectrometry data analysis and interpretation. H.S. initiated the manuscript, and C.J. developed the astrophysical interpretation. All authors actively contributed to multiple versions of the manuscript. The final version was collaboratively written by C.J. and H.S.

Table 1: Examples of assigned chemical formulas for large species (C# ≥ 30) grouped by carbon number (C#) as shown in Figure 3. This selection illustrates the diversity in terms of hydrogenation and presence of heteroatoms (N, O).

Formula	y
$C_{33}H_y$	15-17, 19, 20-22, 24
$C_{33}H_yN$	11, 19, 23, 25, 37
$C_{33}H_{34}OC_{33}H_{25}NO$	34
$C_{33}H_{25}NO$	25
$C_{36}H_y$	14, 16-18, 20-27
$C_{36}H_yN$	15, 21, 25, 39
$C_{36}H_{22}O$	22
$C_{36}H_{25}NO$	25
$C_{40}H_y$	14, 19, 22, 26, 28, 34
$C_{40}H_{21}N$	21
$C_{40}H_{22}O$	22
$C_{42}H_y$	24, 28, 30, 38, 40
$C_{42}HyN$	23, 25
$C_{42}H_{24}O$	24
$C_{45}H_y$	20-22, 24, 30
$C_{45}H_yO$	28, 32
$C_{48}H_y$	16, 23
$C_{48}H_{57}N$	57
$C_{48}H_{46}O$	46
$C_{55}H_y$	30, 31

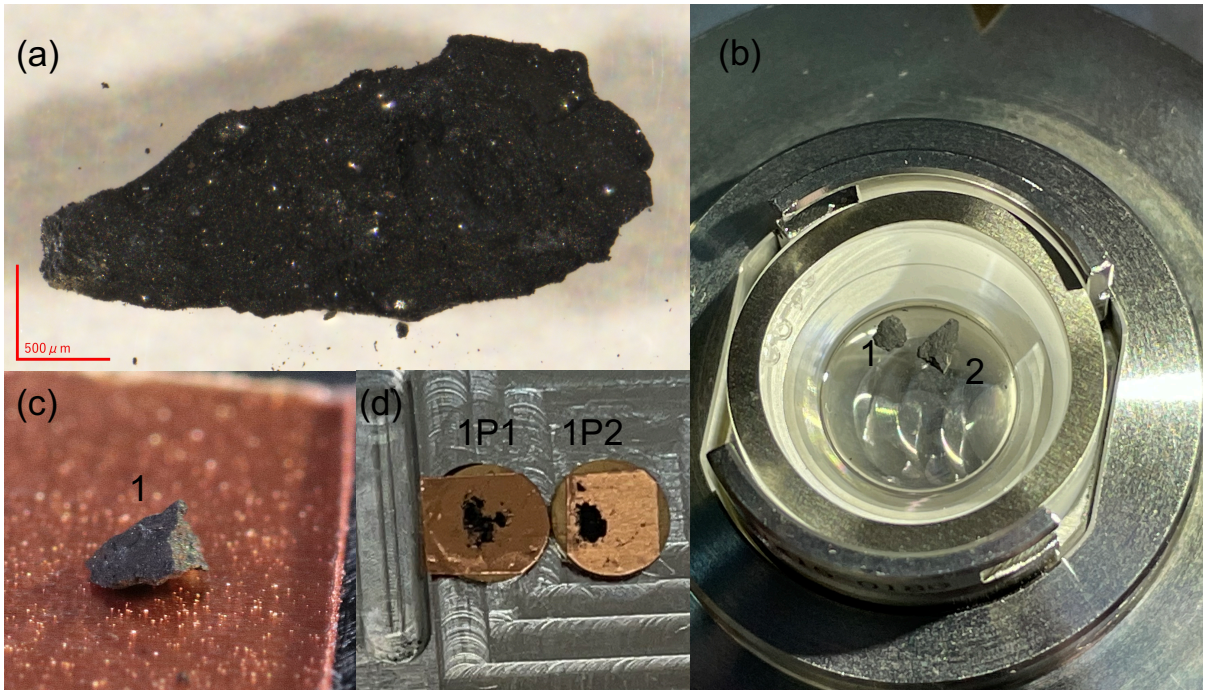

Figure 1: (a) Image of the grain C0083 of Ryugu taken by the JAXA curation center with an optical microscope. (b) Image of the same grain as received at IRAP laboratory. (c) Image of grain C0083_1 sticked on copper double conductive tape for analysis with AROMA. (d) Powder C0083_1P1 (left) and powder C0083_1P2 (right) deposited on double-sided conductive copper tape attached to the AROMA sample holder.

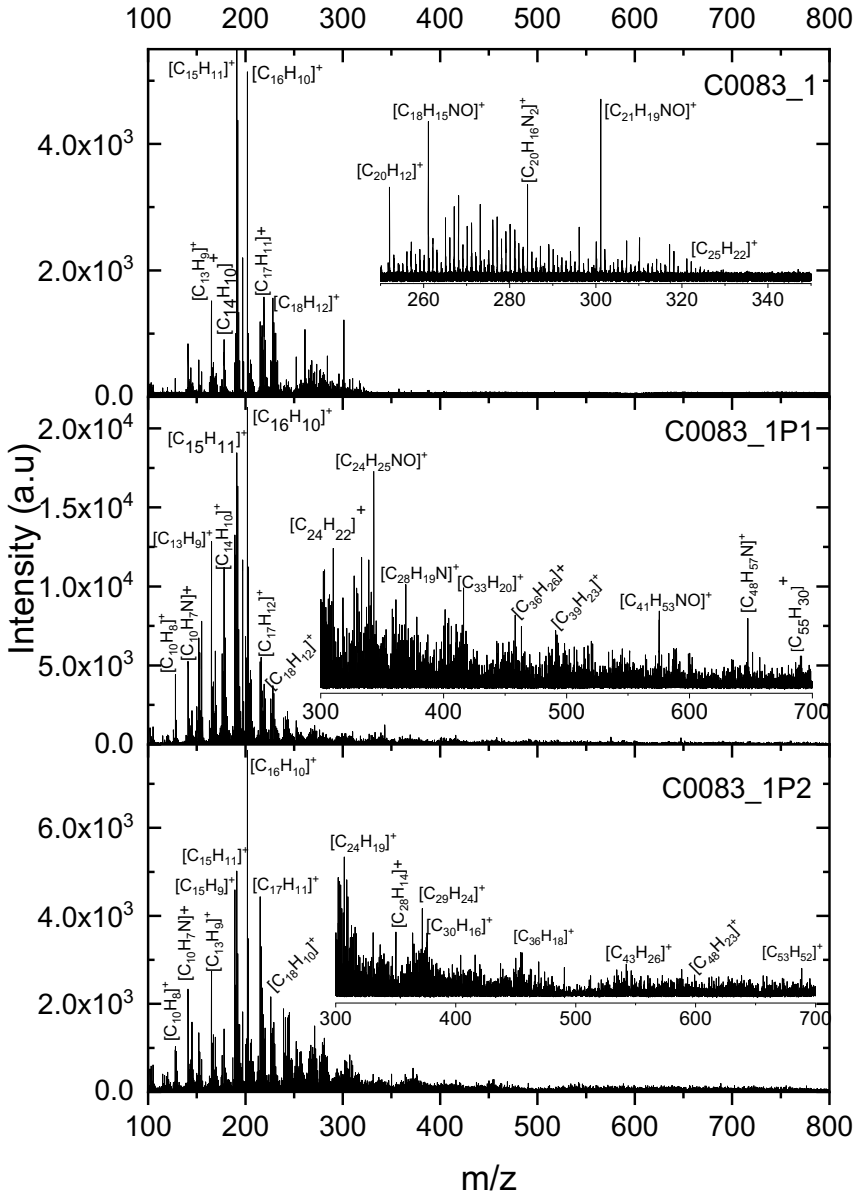

Figure 2: L2MS spectra of Ryugu samples C0083_1, C0083_1P1 and C0083_P2 recorded for positive ions over the (100-800) m/z range. The annotations highlight some of the most common and dominating PAH detected, including ($C_{10}H_8$, $C_{10}H_7N$, $C_{13}H_9$, $C_{14}H_{10}$, $C_{15}H_{11}$, $C_{16}H_{10}$, $C_{17}H_{11}$, $C_{17}H_{12}$, $C_{18}H_{10}$ and $C_{18}H_{12}$). Inset graphs show zoomed-in regions of the mass spectra at high m/z ranges, with additional annotations to highlight large hydrocarbons either pure (i.e. $C_{33}H_{20}$, $C_{36}H_{26}$, $C_{39}H_{23}$, $C_{36}H_{18}$, $C_{43}H_{26}$, $C_{53}H_{52}$, $C_{55}H_{30}$) or containing N and O heteroatoms ($C_{18}H_{15}NO$, $C_{20}H_{16}N_2$, $C_{21}H_{19}NO$, $C_{24}H_{25}NO$, $C_{28}H_{19}N$, $C_{41}H_{53}NO$, $C_{48}H_{57}N$).

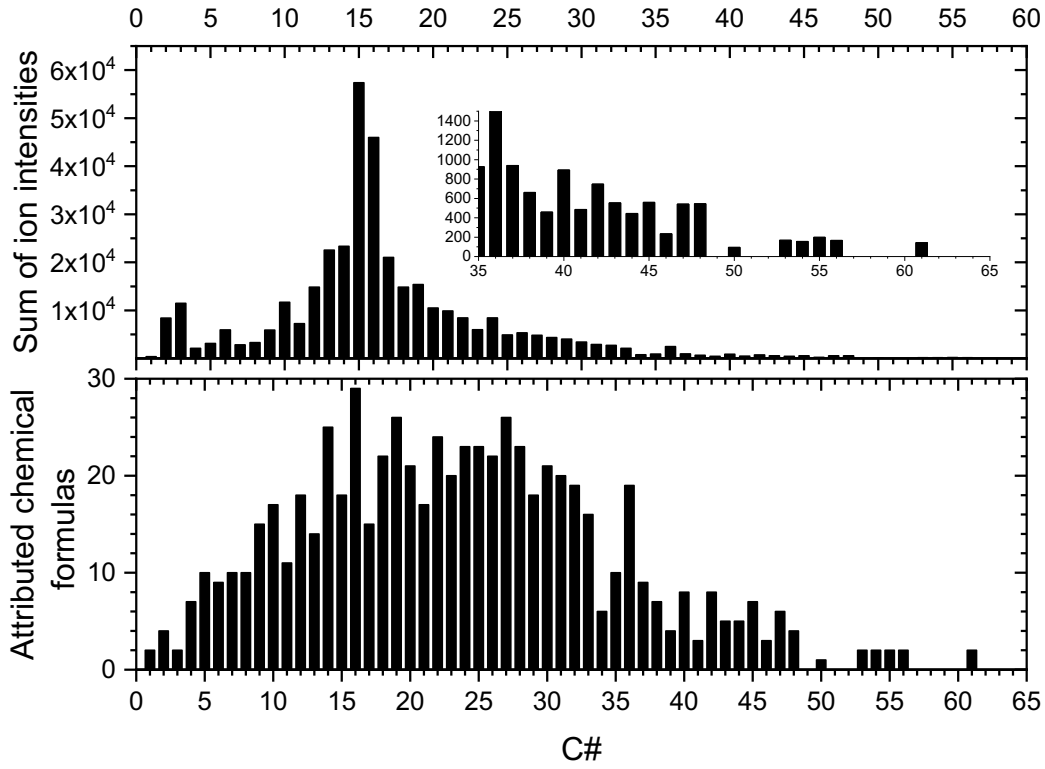

Figure 3: Distribution of species identified in L2MS data of Ryugu samples (data set C0083_1P1P2) grouped per C#. The sum of ion intensities (upper graph) and the total number of attributed chemical formulas (lower graph) are binned and plotted against carbon number (C#).

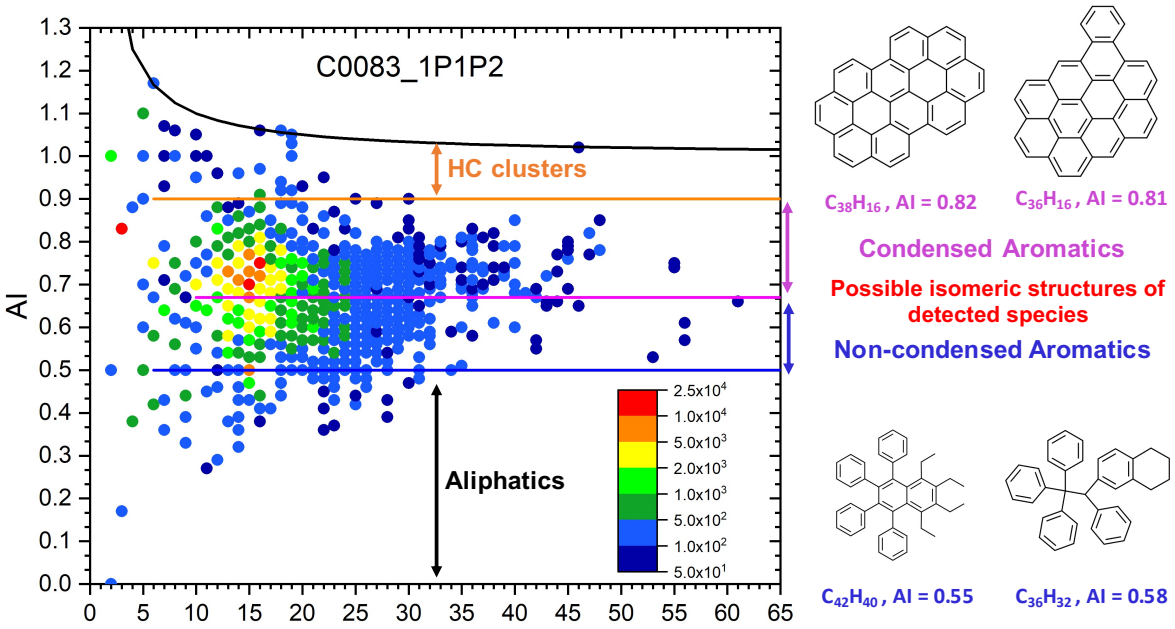

Figure 4: Aromaticity index (AI) analysis of pure hydrocarbon species identified in L2MS data of Ryugu samples (data set C0083_1P1P2). The colored scale on the map represents the absolute ion intensity for each species identified. The solid lines indicate the AI limits used to classify hydrocarbon species into families: aliphatics, non-condensed aromatics, condensed aromatics, and HC clusters. The areas delimiting the families on the graph are highlighted by double-sided coloured arrows. The black lines (AI = 1+1/C#) represent pure carbon species and possibly fullerenes for C#>30. Each species identified is likely to contain a large number of structures. Possible candidate structures are provided for two large non-condensed aromatic and two large condensed aromatic species.

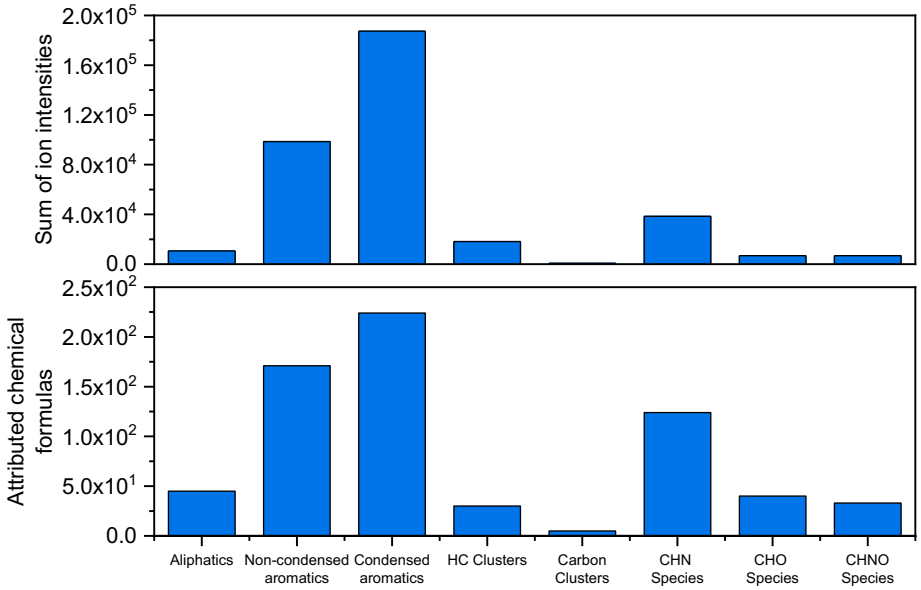

Figure 5: Organic molecule diversity in Ryugu data set C0083_1P1P2 following classification in molecular families. The DBE analysis applied to hydrocarbons allows us to define five carbonaceous families. Three other families are added based on their heteroatom content (N, O). *Upper graph*: sum of ion intensities and *lower graph*: total number of attributed chemical formulas.

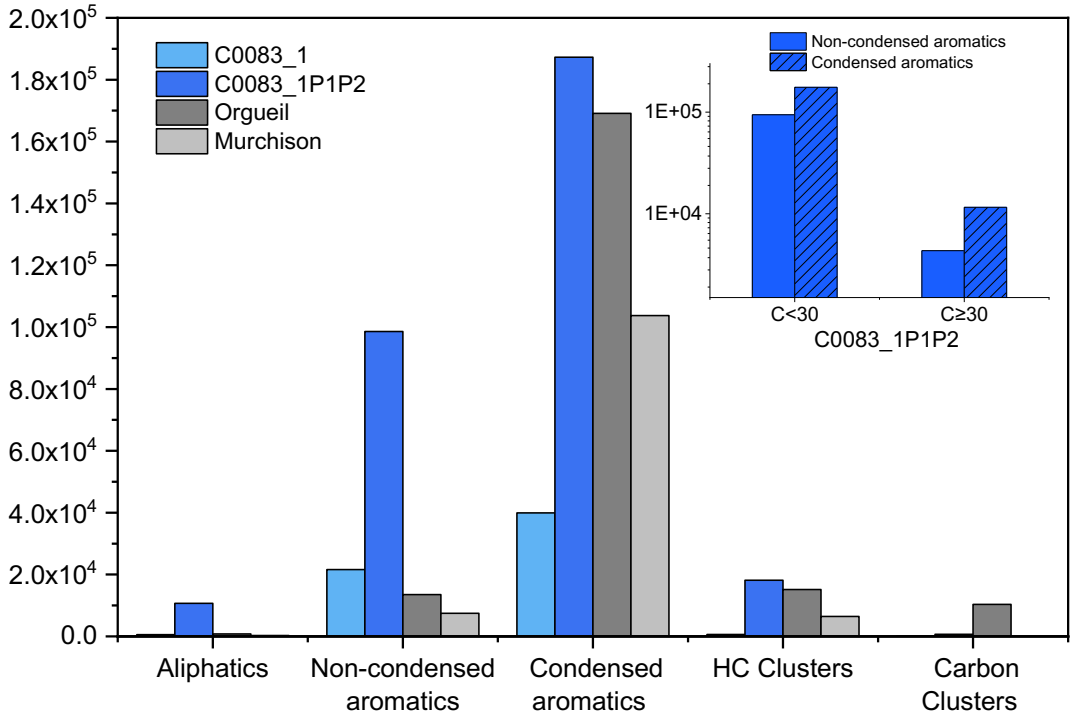

Figure 6: Comparative analysis of carbonaceous molecular families in Ryugu samples and carbonaceous chondrites. The sum of peak intensities is given for the five carbonaceous molecular families identified through the DBE analysis of the L2MS data. The values obtained for Ryugu's intact grain C0083_1 and data set C0083_1P1P2 (in blue) can be compared with the values for Orgueil and Murchison powder samples (in grey). The inset graph highlights the contribution of non-condensed aromatics and condensed aromatics for small to medium ($6 \leq C\# < 30$) and large ($C\# \geq 30$) sizes observed in the C0083 powder samples (data set C0083_1P1P2), with large species observed only in this sample.

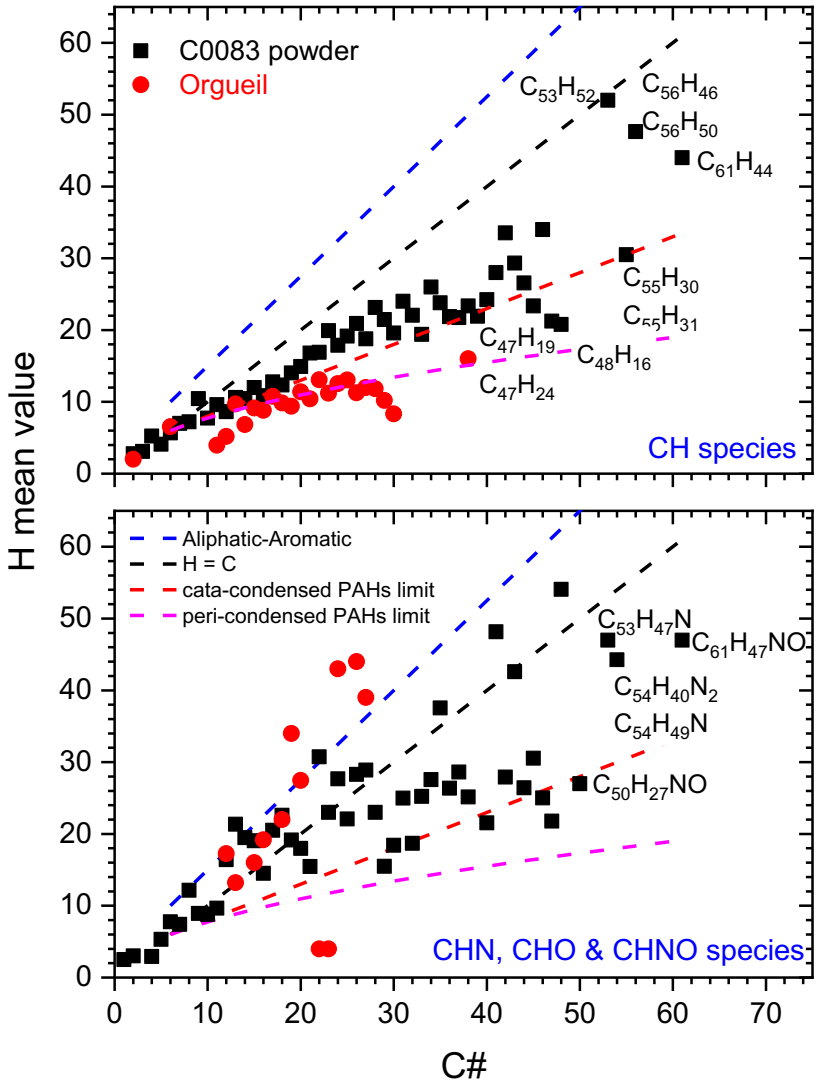

457

458 **Figure 7: H mean value of identified organic species per C#.** The H mean value is calculated
459 by summing the weighted number of hydrogen atoms (H) for each species identified, taking
460 into account its absolute intensity. The total is then divided by the number of species detected.
461 The upper graph shows the H mean value for pure hydrocarbon (CH) in two samples, Orgueil
462 and the data set C0083_1P1P2. The lower graph shows the H mean value for CHN, CHO and
463 CHNO species in both samples. Empirical limits are indicated for aliphatic/aromatic
464 hydrocarbons (dashed blue line), cata-condensed PAHs (dashed red line), and peri-condensed
465 PAHs (dashed pink line)[47], along with the H = C black dashed line for reference.

466

467

REFERENCES:

1. Nakamura, T., Matsumoto, M., Amano, K., *et al.* Formation and evolution of carbonaceous asteroid Ryugu: Direct evidence from returned samples. *Science* **379**, 787 (2023).
2. Naraoka, H., Takano, Y., Dworkin, J. P., *et al.* Soluble organic molecules in samples of the carbonaceous asteroid (162173) Ryugu. *Science* **379**, 789 (2023).
3. Yokoyama, T., Nagashima, K., Nakai, I., *et al.* Samples returned from the asteroid Ryugu are similar to Ivuna-type carbonaceous meteorites. *Science* **379**, 786 (2022).
4. Potiszil, C., Ota, T., Yamanaka, M., *et al.* Insights into the formation and evolution of extraterrestrial amino acids from the asteroid Ryugu. *Nat Commun* **14**, 1482 (2023).
5. Yabuta, H. Macromolecular organic matter in samples of the asteroid (162173) Ryugu. (2023).
6. Peeters, E. Astronomical observations of the PAH emission bands. *EAS Publications Series* **46**, 13–27 (2011).
7. Li, A. Spitzer's perspective of polycyclic aromatic hydrocarbons in galaxies. *Nat Astron* **4**, 339–351 (2020).
8. Chown, R., Sidhu, A., Peeters, E., *et al.* PDRs4All IV. An embarrassment of riches: Aromatic infrared bands in the Orion Bar. *A&A* (2023) doi:10.1051/0004-6361/202346662.
9. Montillaud, J., Joblin, C. & Toublanc, D. Evolution of polycyclic aromatic hydrocarbons in photodissociation regions - Hydrogenation and charge states. *A&A* **552**, A15 (2013).
10. Wenzel, G., Joblin, C., Giuliani, A., *et al.* Astrochemical relevance of VUV ionization of large PAH cations. *Astronomy & Astrophysics* **641**, A98 (2020).

11. Cernicharo, J., Agúndez, M., Cabezas, C., *et al.* Pure hydrocarbon cycles in TMC-1: Discovery of ethynyl cyclopropenylidene, cyclopentadiene, and indene. *A&A* **649**, L15 (2021).
12. Burkhardt, A. M., Lee, K. L. K., Changala, P. B., *et al.* Discovery of the Pure Polycyclic Aromatic Hydrocarbon Indene (c-C9H8) with GOTHAM Observations of TMC-1. *ApJL* **913**, L18 (2021).
13. McGuire, B. A., Loomis, R. A., Burkhardt, A. M., *et al.* Detection of two interstellar polycyclic aromatic hydrocarbons via spectral matched filtering. *Science* **371**, 1265–1269 (2021).
14. Joblin, C. & Cernicharo, J. Detecting the building blocks of aromatics. *Science* **359**, 156–157 (2018).
15. Pizzarello, S. & Shock, E. The Organic Composition of Carbonaceous Meteorites: The Evolutionary Story Ahead of Biochemistry. *Cold Spring Harbor Perspectives in Biology* **2**, a002105–a002105 (2010).
16. Sephton, M. A. Organic matter in carbonaceous meteorites: past, present and future research. *Phil. Trans. R. Soc. A.* **363**, 2729–2742 (2005).
17. Sephton, M. A. Organic compounds in carbonaceous meteorites. *Nat. Prod. Rep.* **19**, 292–311 (2002).
18. Nittler, L. R. & Ciesla, F. Astrophysics with Extraterrestrial Materials. *Annual Review of Astronomy and Astrophysics* **54**, 53–93 (2016).
19. Berné, O., Cox, N. L. J., Mulas, G. & Joblin, C. Detection of Buckminsterfullerene emission in the diffuse interstellar medium. *Astron Astrophys* **605**, L1 (2017).
20. Cami, J., Bernard-Salas, J., Peeters, E. & Malek, S. E. Detection of C_{60} and C_{70} in a Young Planetary Nebula. *Science* **329**, 1180–1182 (2010).

21. Campbell, E. K., Holz, M. & Maier, J. P. C60+ in diffuse clouds: laboratory and astronomical comparaison. *ApJL* **826**, L4 (2016).
22. Sabbah, H., Carlos, M., Jenniskens, P., *et al.* Detection of Cosmic Fullerenes in the Almahata Sitta Meteorite: Are They an Interstellar Heritage? *ApJ* **931**, 91 (2022).
23. Sabbah, H., Bonnamy, A., Papanastasiou, D., *et al.* Identification of PAH Isomeric Structure in Cosmic Dust Analogs: The AROMA Setup. *ApJ* **843**, 34 (2017).
24. Sabbah, H., Commodo, M., Picca, F., *et al.* Molecular content of nascent soot: Family characterization using two-step laser desorption laser ionization mass spectrometry. *Proceedings of the Combustion Institute* **38**, 1241–1248 (2021).
25. Bérard, R., Makasheva, K., Demyk, K., *et al.* Impact of Metals on (Star)Dust Chemistry: A Laboratory Astrophysics Approach. *Front. Astron. Space Sci.* **8**, 654879 (2021).
26. Müller, W. H., Verdin, A., De Pauw, E., Malherbe, C. & Eppe, G. Surface-assisted laser desorption/ionization mass spectrometry imaging: A review. *Mass Spectrom Rev* **41**, 373–420 (2022).
27. Strohalm, M., Kavan, D., Novák, P., Volný, M. & Havlíček, V. *mMass* 3: A Cross-Platform Software Environment for Precise Analysis of Mass Spectrometric Data. *Anal. Chem.* **82**, 4648–4651 (2010).
28. Marshall, A. G. & Rodgers, R. P. Petroleomics: Chemistry of the underworld. *Proc. Natl. Acad. Sci. U.S.A.* **105**, 18090–18095 (2008).
29. Koch, B. P. & Dittmar, T. From mass to structure: an aromaticity index for high-resolution mass data of natural organic matter. *Rapid Commun. Mass Spectrom.* **20**, 926–932 (2006).
30. Hsu, C. S., Lobodin, V. V., Rodgers, R. P., McKenna, A. M. & Marshall, A. G. Compositional Boundaries for Fossil Hydrocarbons. *Energy Fuels* **25**, 2174–2178 (2011).

31. Kitazato, K., Milliken, R. E., Iwata, T., *et al.* The surface composition of asteroid 162173 Ryugu from Hayabusa2 near-infrared spectroscopy. *Science* **364**, 272–275 (2019).
32. Sugita, S., Honda, R., Morota, T., *et al.* The geomorphology, color, and thermal properties of Ryugu: Implications for parent-body processes. *Science* **364**, eaaw0422 (2019).
33. Aponte, J. C., Dworkin, J. P., Glavin, D. P., *et al.* PAHs, hydrocarbons, and dimethylsulfides in Asteroid Ryugu samples A0106 and C0107 and the Orgueil (CI1) meteorite. *Earth, Planets and Space* **75**, 28 (2023).
34. Zeichner, S. S., Aponte, J. C., Bhattacharjee, S., *et al.* Polycyclic aromatic hydrocarbons in samples of Ryugu formed in the interstellar medium. *Science* **382**, 1411–1416 (2023).
35. Yabuta, H., Cody, G. D., Engrand, C., *et al.* Macromolecular organic matter in samples of the asteroid (162173) Ryugu. *Science* **379**, eabn9057 (2023).
36. Lecasble, M., Bernard, S., Viennet, J.-C., Criouet, I. & Remusat, L. Influence of hydrothermal asteroidal conditions on the molecular structure and isotopic compositions of polycyclic aromatic hydrocarbons. *Icarus* **401**, 115603 (2023).
37. Kebukawa, Y., Quirico, E., Dartois, E., *et al.* Infrared absorption spectra from organic matter in the asteroid Ryugu samples: Some unique properties compared to unheated carbonaceous chondrites. *Meteoritics & Planetary Science* **n/a**,.
38. Danger, G., Ruf, A., Maillard, J., *et al.* Unprecedented Molecular Diversity Revealed in Meteoritic Insoluble Organic Matter: The Paris Meteorite's Case. *Planet. Sci. J.* **1**, 55 (2020).
39. Laurent, B., Maillard, J., Afonso, C., *et al.* Diversity of chondritic organic matter probed by ultra-high resolution mass spectrometry. *Geochem. Persp. Let.* **22**, 31–35 (2022).
40. Zhao, L., Kaiser, R. I., Xu, B., *et al.* Pyrene synthesis in circumstellar envelopes and its role in the formation of 2D nanostructures. *Nat Astron* **2**, 413–419 (2018).

41. Cherchneff, I., Barker, J. R. & Tielens, A. G. G. M. Polycyclic Aromatic Hydrocarbon Formation in Carbon-rich Stellar Envelopes. *The Astrophysical Journal* **401**, 269 (1992).
42. Frenklach, M. & Feigelson, E. D. Formation of polycyclic aromatic hydrocarbons in circumstellar envelopes. *ApJ* **341**, 372 (1989).
43. Nittler, L. R. Presolar stardust in meteorites: recent advances and scientific frontiers. *Earth and Planetary Science Letters* **209**, 259–273 (2003).
44. Martínez, L., Santoro, G., Merino, P., *et al.* Prevalence of non-aromatic carbonaceous molecules in the inner regions of circumstellar envelopes. *Nat Astron* **4**, 97–105 (2019).
45. Pilleri, P., Montillaud, J., Berné, O. & Joblin, C. Evaporating very small grains as tracers of the UV radiation field in photo-dissociation regions. *A&A* **542**, A69 (2012).
46. Pilleri, P., Joblin, C., Boulanger, F. & Onaka, T. Mixed aliphatic and aromatic composition of evaporating very small grains in NGC 7023 revealed by the 3.4/3.3 μm ratio. *A&A* **577**, A16 (2015).
47. Cain, J., Laskin, A., Kholghy, M. R., Thomson, M. J. & Wang, H. Molecular characterization of organic content of soot along the centerline of a coflow diffusion flame. *Phys. Chem. Chem. Phys.* **16**, 25862–25875 (2014).